Spectral weight and thermodynamic properties of $YBa_2Cu_3O_{6+x}$ thin films

2006 J. Phys.: Condens. Matter 18 8161

(http://iopscience.iop.org/0953-8984/18/35/004)

INSTITUTE OF PHYSICS PUBLISHING JOURNAL OF PHYSICS: CONDENSED MATTER

J. Phys.: Condens. Matter **18** (2006) 8161–8168 doi:10.1088/0953-8984/18/35/004

Spectral weight and thermodynamic properties of $YBa_2Cu_3O_{6+x}$ thin films

A El Azrak[1], M Zazoui[1], I Zorkani[2], M Hamedoun[2] and N Bontemps[3]

[1] Laboratoire de Physique de la Matière Condensée, Faculté des Sciences et Techniques Mohammédia, B.P. 146 Mohammédia, Morocco
[2] Laboratoire de Physique du Solide, Faculté des Sciences Fès, B.P. 1976, Fès, Morocco
[3] Laboratoire de Physique du Solide, ESPCI (UPR5 CNRS), 75231 Paris Cedex 05, France

E-mail: aea_elazrak@yahoo.fr

Received 14 March 2006, in final form 19 June 2006
Published 15 August 2006
Online at stacks.iop.org/JPhysCM/18/8161

Abstract

The ab-plane reflectivity of $YBa_2Cu_3O_{6+x}$ thin films was measured in the 500–25 000 cm^{-1} range in samples with $x = 1$ ($T_c = 90$ K), $x = 0.85$ ($T_c = 82$ K), $x = 0.6$ ($T_c = 55$ K), $x = 0.45$ ($T_c = 35$ K) and $x = 0.38$ ($T_c = 20$ K) in normal state. The effective charge carrier number obtained from the spectral weight increases with increasing x. Variation is consistent with higher d_c resistivity for $x < 0.45$. On the other hand the scattering frequency dependent rate shows significant differences between optimally oxygen doped and underdoped material. Results show that the high-T_c superconductor normal state deviates in many fundamental aspects from conventional superconductors.

1. Introduction

Since the discovery of the high temperature superconductivity (HTSC), considerable efforts have been made to describe and understand superconducting phase response. HTSC continues to present some of the biggest challenges in materials science. Over the years, measurements have been carried out in larger temperature and doping ranges, hoping to get a new insight into the problem.

Electron-doped cuprate [1] discovery gave access to the mirror image of the hole-doped phase diagram with respect to the Mott insulator state. Since then, significant work has been done looking for differences and similarities in each kind of charge carrier system. The electron and hole doped cuprate phase diagram shows a global symmetry. However, many electron doped compound aspects, including the superconducting gap nature, the behaviour of the normal state charge carriers, and the presence of a normal state gap (pseudo-gap), are still unclear.

The main results from infrared spectroscopy can be summarized as follows [2–6]:

- it is generally believed that the cuprate superconductor normal state is not a Fermi liquid;

- various anomalous behaviours have been discovered beyond BCS theory standard. One of them is the pseudo-gap (PG) observed in the material normal state, which has aroused a great deal of controversy about the relationship between the pseudo-gap and the superconducting state. The angle-resolved photoemission spectroscopy (ARPES) has suggested that the PG is the paired precursor state of the superconducting coherence. The other, however, considers it only as a competing or coexisting order with the superconductivity.

The only consensus on the normal state of HTSC electronic properties is that they are not conventional. All models describing cuprate normal state assume a strong electron–electron and electron–phonon interaction.

The disorder introduced by cationic or oxygen doping influences the spectrum of excitations, making the physics of the system more complex. The problems that have been discussed for many years recently are the relevance of disorder to localization and localization to superconductivity, in particular near the metal–insulator transition [7, 8]. In cuprates, this could apply to a strongly underdoped material. Another twist appears when observing a normal state gap in underdoped cuprates [9, 10]. It was first observed as a pseudo-gap in NMR data, and later associated with the departure from the linear dependence on resistivity.

The infrared response (IR) may be characterized by two contributions: a low frequency, Drude-like behaviour assigned to free charge carriers, and a strong midinfrared contribution (the midinfrared band or MIB) [11, 12].

So far, the MIB origin is not yet clear. Generalized Drude conductivity, where both effective mass and relaxation time of normal state charge carriers are frequency dependent, appears to be an alternative description of infrared response [13]. This single component approach was promoted later through experimental analyses, showing that relaxation rate exhibits a linear variation with frequency in a large frequency domain, up to 2000 cm^{-1} on the single domain YBCO crystal [14], and even 6000 cm^{-1} on the Bi-based single crystal [15]. The infrared conductivity data of YBCO and BSCO thin films derived from reflectivity spectra extending up to 25 000 cm^{-1} show the following [16, 17].

(i) The linear variation of the relaxation rate $1/\tau$ versus frequency extends up to 6000 cm^{-1} and $1/\tau$ is the same for all optimally doped compounds.
(ii) In the 1000–6000 cm^{-1} range, the temperature change of the transmission from 90 to 300 K can only be quantitatively accounted for by a linear variation of the relaxation rate with temperature. These results are consistent with the marginal Fermi liquid model (MFL) [18].

Our paper concentrates on room-temperature reflectivity data, on a set of $YBa_2Cu_3O_{6+x}$ thin films, for $0.38 < x < 1$. We observe that the reflectivities of our identified best $YBa_2Cu_3O_{6+x}$ ($x = 0.38, 0.45, 0.60, 0.85, 1$) samples are very high, compared to the reflectivity associated with the $YBa_2Cu_3O_{6+x}$ crystal [12]. In this work we show a direct connection between the real part of the conductivity $\sigma(\omega)$ obtained by Kramers–Kronig (KK) analysis and the low energy excitation. We also show the importance of studying the high-T_c superconductor as a function of the free charge carrier concentration.

2. Experiment

2.1. Sample preparation and characterization

One single 15 × 15 mm^2 (3000 ± 200) Å thick film has been prepared by laser ablation [19]. We noted that it shows an epitaxial growth with respect to the MgO axes with a partial 45° well

known orientation. This film was cut into six pieces and each of them checked by four point resistivity measurements and reflectivity. On this basis, one sample was discarded. The other five exhibited a very similar behaviour: $\rho(T)$ goes linearly to $\sim$ zero ($d\rho/dT = 1\ \mu\Omega\,\mathrm{cm\,K^{-1}}$) at $T_c \sim 90$ K. The room temperature reflectivities were identical within $\pm 2\%$, and, below 2000 $\mathrm{cm^{-1}}$, lower (by 5%) than the standard one [16].

One piece was kept at $x = 1$, while the others were annealed at controlled temperature and oxygen pressure in order to achieve various oxygen contents $x = 0.85, 0.6, 0.45, 0.38$. The samples were then checked by x-ray diffraction and optical measurements were performed. The five $YBa_2Cu_3O_{6+x}$ samples which we have studied are labelled as follows:

A: $YBa_2Cu_3O_7$ on MgO, $7.5 \times 5\ \mathrm{mm^2}$, 3000 Å, $T_c \sim 90$ K
B: $YBa_2Cu_3O_{6.85}$ on MgO, $7.5 \times 5\ \mathrm{mm^2}$, 3000 Å, $T_c \sim 82$ K
C: $YBa_2Cu_3O_{6.60}$ on MgO, $7.5 \times 5\ \mathrm{mm^2}$, 3000 Å, $T_c \sim 55$ K
D: $YBa_2Cu_3O_{6.45}$ on MgO, $7.5 \times 5\ \mathrm{mm^2}$, 3000 Å, $T_c \sim 35$ K
E: $YBa_2Cu_3O_{6.38}$ on MgO, $7.5 \times 5\ \mathrm{mm^2}$, 3000 Å, $T_c \sim 20$ K.

2.2. Experimental methods

Reflectivity near normal incidence has been recorded in the 500–7000 $\mathrm{cm^{-1}}$ spectral range with an IFS66 Bruker Fourier-transform spectrometer and in the 5000–25 000 $\mathrm{cm^{-1}}$ range with a Cary 17 spectrophotometer. In order to measure absolute reflectivity, we used as unit reflectivity references a gold mirror in the infrared range and a silver mirror in the visible frequency. Our accuracy to determine absolute reflectivity is better than 1%.

2.3. Kramers–Kronig transformations

Kramers–Kronig analysis from reflectivity data has been used in order to establish the dielectric functions and the real part of the conductivity. Our sample thickness is high (3000 Å) so there is no significant contribution from the substrate to the reflected flux. It is noted that the reflectivity spectrum of pure MgO exhibits a pronounced dip at 1000 $\mathrm{cm^{-1}}$ and the same dip is clearly displayed on our films. We have therefore decided to run the Kramers–Kronig analysis from reflectivity spectra.

We calculated the phase $\theta(\omega_i)$ of the complex reflectance coefficient by KK transformations of the measured the reflectivity spectrum:

$$\theta(\omega_i) = \frac{\omega_i}{\pi} \int_0^{+\infty} \frac{\ln R(\omega_i) - \ln R(\omega)}{\omega^2 - \omega_i^2}\, d\omega. \tag{1}$$

The knowledge of R and θ allows the determination of the optical function (the dielectric functions, the real part of the conductivity $\sigma, \ldots$).

Experimentally the reflectivity is only known within a spectral range (ω_b, ω_h). We have chosen the Hagen–Rubens relation to extrapolate low frequency data:

$$R(\omega) = 1 - (1 - R_b)\sqrt{\frac{\omega}{\omega_b}} \tag{2}$$

where R_b is the reflectivity at ω_b. High energy termination is more delicate. We have then assumed for the high frequency termination $\omega > \omega_h$:

$$R(\omega) = R(\omega_h)(\omega_h/\omega)^p \tag{3}$$

and we have adjusted the exponent (p) in order to smoothly fit the reflectivity spectrum.

It is easy to show that the contribution to the phase $\theta(\omega_i)$ arising from the $\omega \gg \omega_i$ frequencies involves a term of the order of ω_i/ω and therefore decreases strongly any weight due to the actual high frequency reflectivity.

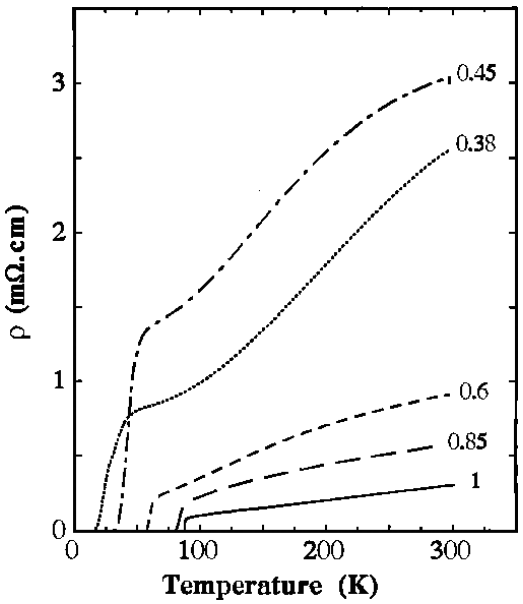

Figure 1. Resistivity of $YBa_2Cu_3O_{6+x}$ thin films as a function of temperature. Deviation in the linear resistivity behaviour is observed for the underdoped material.

3. Results and discussion

3.1. Resistivity

Figure 1 shows resistivity spectra of the films set as a function of temperature. Qualitatively, resistivity changes (occurrence of an upward curvature for $x \leqslant 0.6$ near T_c and increase of $\rho(T)$ as x decreases) are similar to what is expected [19]. Quantitatively, only $x = 1$ and $x = 0.85$ exhibit the proper behaviour.

3.2. Reflectivity

The reflectivity spectra (R) are measured in the range 500–30 000 cm^{-1} at 300 K, for the five $YBa_2Cu_3O_{6+x}$ samples: A, B, C, D and E with different x ($x = 1$, 0.85, 0.60, 0.45 and 0.38). Previously, it has been shown in crystals [10] and in ceramics [11] that reflectivity in the $YBa_2Cu_3O_{6+x}$ family of compounds is extremely sensitive to oxygen concentration. A comparison of the reflectivity of sample A with published reflectivity of an untwined $YBa_2Cu_3O_7$ crystal, for the electric field polarized parallel to the a-axis or to the b-axis, shows that our films exhibit a very high quality. Spectra in figure 2 display an apparent plasma frequency decrease as x decreases. Note that the spectrum dip at $\sim$1000 cm^{-1} is due to the MgO substrate.

3.3. Conductivity

Conductivity spectra σ, derived from a Kramers–Kronig analysis of spectrum reflectivity, are plotted in figure 3. The behaviour of σ as a function of oxygen content plays a crucial role in identifying the contribution to free charge carriers, as opposed to the contribution from band electrons.

The conductivity spectra increase with increasing x; however, the growth rate is not uniform. Spectral weight increases most rapidly for $\omega < 4000$ cm^{-1}, and is nearly independent of oxygen content for $\omega > 8000$ cm^{-1}. We show that infrared response may be characterized

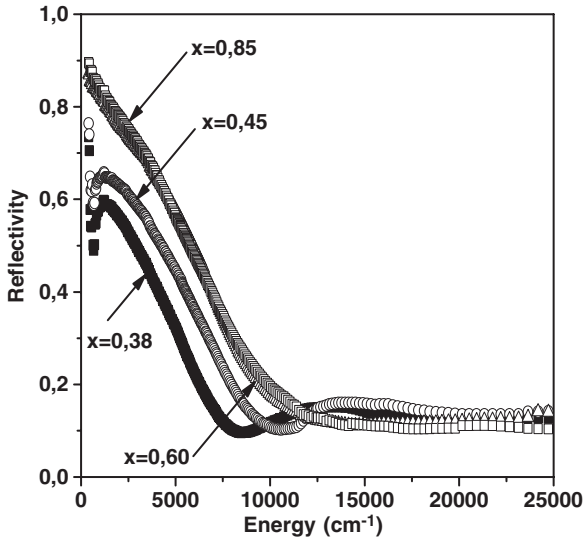

Figure 2. Reflectivity spectra of $YBa_2Cu_3O_{6+x}$ thin films as a function of frequency.

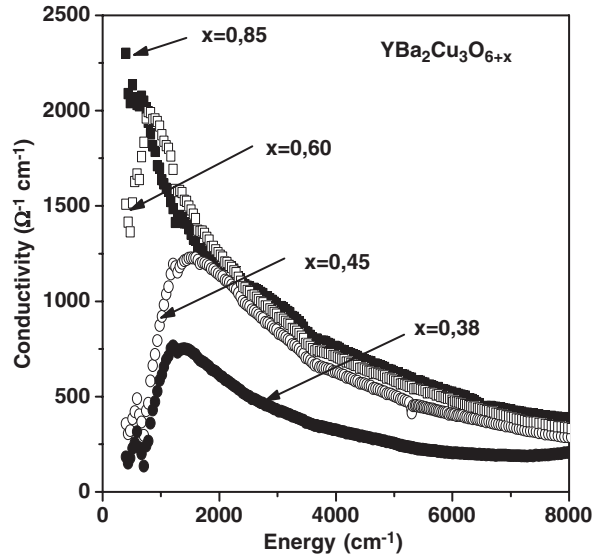

Figure 3. Optical conductivity σ of $YBa_2Cu_3O_{6+x}$ thin films as a function of frequency. These curves are obtained from a Kramers–Kronig transformation of the data in figure 2.

by two contributions: a low frequency, Drude-like behaviour assigned to free charge carriers, and a strong midinfrared contribution associated with band electrons.

3.4. Scattering rate $1/\tau$

The generalized Drude conductivity, where both effective mass and relaxation time of normal state charge carriers are frequency dependent, appears to be an alternative description of the infrared response.

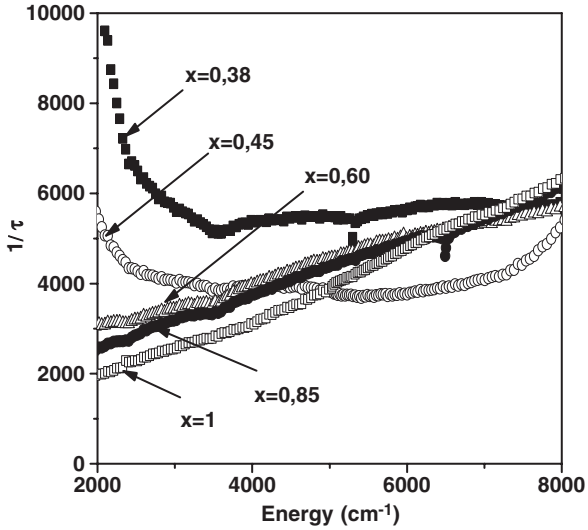

Figure 4. Relaxation rate of the charge carriers from the $YBa_2Cu_3O_{6+x}$ thin films. The complicated frequency dependence of the relaxation rate $1/\tau$ is consistent with the deviation in the linearity of the resistivity versus temperature.

We show the frequency dependence of the relaxation rate $1/\tau$ in figure 4. The noteworthy result here is that relaxation rate exhibits a linear dependence for optimally doped compounds ($x > 0.85$). We recover standard linear behaviour [16, 17].

In underdoped or strongly underdoped materials, the frequency dependent scattering rate shows some significant differences from optimally oxygen doped material. This is consistent with the discrepancy observed in the $\rho(T)$ data (figure 1).

We thus conclude that although quantitative behaviour remains to be established, we observe a well defined qualitative trend on scattering rate. Its linear behaviour extends on a more restricted frequency range, which may be correlated with the linearity loss of the resistivity.

4. Layered electron gas

It has been argued, relying essentially on the experimental observation that the frequency dependence of $\mathrm{Im}\,(-1/\varepsilon)$ is quadratic, that non-Drude behaviour may be characteristic of a layered electron gas [20, 21].

We have reported $\mathrm{Im}(-1/\varepsilon)$ versus frequency in figure 5.

We found that the maximum of $\mathrm{Im}(-1/\varepsilon)$ associated with a plasma frequency increases with increasing x.

For $x > 0.85$, $\mathrm{Im}(-1/\varepsilon)$ versus frequency is quadratic as compared to optimally doped superconducting material. We found that $\mathrm{Im}(-1/\varepsilon)$ departs from its quadratic variation at lower frequencies as x decreases, in correlation with the absence of linearity in $\rho(T)$ versus temperature.

4.1. Effective charge carrier number $N_{\mathrm{eff}}(\omega)$, and plasma frequency ω_p

N_{eff} is defined according to the relation

$$N_{\mathrm{eff}}(\omega) = \frac{2mV}{\pi e^2} \int_0^{\omega} \sigma(\omega')\,\mathrm{d}\omega' \tag{4}$$

where e and m are respectively bare electronic charge and mass, and V is the unit-cell volume.

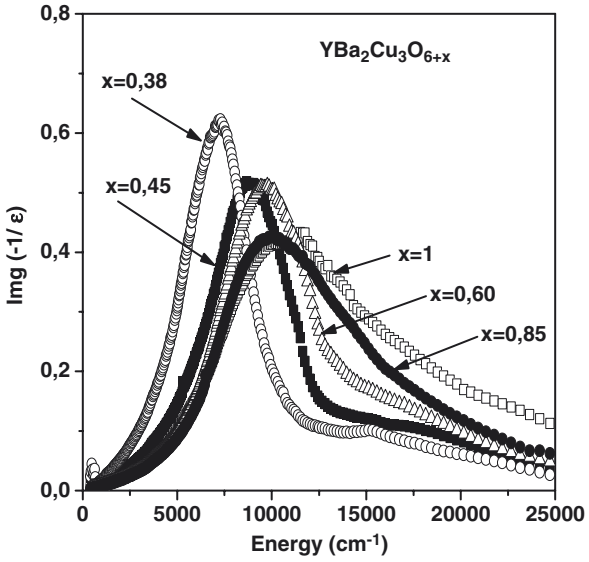

Figure 5. Im $(-1/\varepsilon)$ versus frequency of the various samples.

The significance of $N_{\text{eff}}(\omega)$ may be appreciated by considering the sum rule on the conductivity:

$$\int_0^{+\infty} \sigma(\omega)\,\mathrm{d}\omega = \frac{\pi n e^2}{2m} \simeq \frac{\omega_p^2}{8} \tag{5}$$

where n is the total density of electrons. N_{eff} can be converted to an equivalent plasma frequency ω_p through the relation [22]

$$\omega_p^2 e V^2 = \frac{4\pi e^2}{m}\frac{N_{\text{eff}}}{V} = 7.95 N_{\text{eff}}. \tag{6}$$

Figure 6 shows the $N_{\text{eff}}(\omega)$ of the $YBa_2Cu_3O_{6+x}$ thin films as a function of x, at various frequencies (800, 2000 and 8000 cm^{-1}). When varying the oxygen amount x from a strongly underdoped ($x = 0.38$; $T_c = 20$ K) to an optimally doped ($x = 1$; $T_c = 90$ K), we find that the N_{eff} or plasma frequency increases with doping and frequency.

5. Conclusion

In this paper we report measurements and analysis of the conductivity $\sigma(\omega)$ of $YBa_2Cu_3O_{6+x}$ thin films as a function of frequency. We show that infrared response may be characterized by two contributions: a low frequency, Drude-like behaviour assigned to free charge carriers, and a strong midinfrared contribution associated with band electrons.

The spectral weight of this conductivity increases with increasing x. However, the growth rate is not uniform. The spectral weight increases for $\omega < 4000$ cm^{-1}, and is nearly independent of oxygen content for $\omega > 8000$ cm^{-1}.

On the other hand, we show that the spectrum of N_{eff} is not consistent with the sum rule (equation (5)) for charge carriers density and band mass. N_{eff} increases with increasing oxygen concentration (x), and frequency up to 1 eV. It was consistent with the remainder of N_{eff} that we expected from the hole-density and band mass [23–25].

We conclude that the complicated frequency dependence of the relaxation rate $1/\tau$, and the deviation in the linearity of the resistivity versus temperature, suggests that free charge carriers

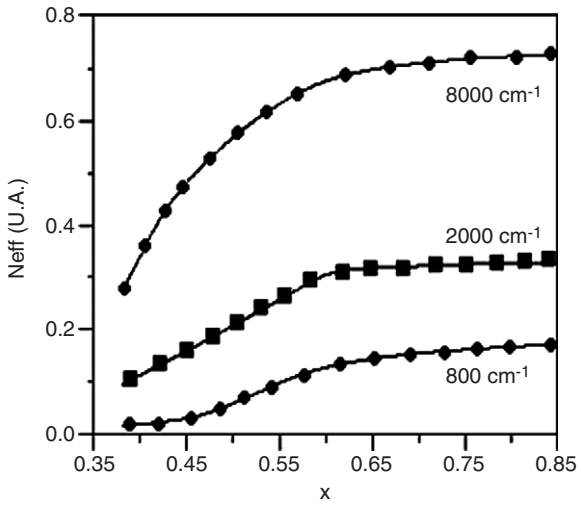

Figure 6. N_{eff} as a function of x at various frequencies (800, 2000 and 8000 cm^{-1}). The data are obtained by integrating the conductivity curves up to 8000 cm^{-1} (equation (4)).

interact significantly with other excitations of material. Finally, the electronic correlation nature in the normal state determines the different aspects of the superconductivity in these materials [26].

References

[1] Takagi H, Uchida S and Tokura Y 1989 *Phys. Rev. Lett.* **62** 1197
[2] Timusk T and Statt B 1999 *Rep. Prog. Phys.* **62** 61
[3] Orenstein J *et al* 1990 *Phys. Rev.* B **42** 6342
[4] Basov D N *et al* 1994 *Phys. Rev.* B **49** 12165
[5] Santander-Syro A F *et al* 2003 *Europhys. Lett.* **62** 568
[6] Homes C C *et al* 2004 *Phys. Rev.* B **69** 24514
[7] Huscroft C and Scalettar R T 1998 *Phys. Rev. Lett.* **81** 1775
[8] Sadovskii M V 1997 *Phys. Rep.* **282** 225
[9] Puchkov A V *et al* 1996 *J. Phys.: Condens. Matter* **8** 10049
[10] Renner C *et al* 1998 *Phys. Rev. Lett.* **80** 149
[11] Timusk T *et al* 1990 *Physica* C **169** 425
[12] Orenstein J *et al* 1990 *Phys. Rev.* B **42** 6342
[13] Schlesinger Z *et al* 1990 *Phys. Rev. Lett.* **41** 801
[14] Terasaki I *et al* 1991 *Physica* C **185–189** 1017
[15] Varma C M *et al* 1989 *Phys. Rev. Lett.* **63** 1996
[16] El Azrak A *et al* 1994 *Phys. Rev.* B **49** 9846
[17] El Azrak A *et al* 1993 *J. Alloys Compounds* **195** 663
[18] Littlewood P B *et al* 1991 *J. Appl. Phys.* **69** 4979
[19] Wuyts B *et al* 1993 *Phys. Rev.* B **47** 5512
[20] Bozovic I 1990 *Phys. Rev.* B **42** 1969
[21] Bozovic I *et al* 1991 *Phys. Rev.* B **43** 1169
[22] Stern F 1963 *Solid State Physique* vol 15 (New York: Academic)
[23] Homes C C *et al* 2004 *Phys. Rev.* B **69** 024514
[24] Santander-Syro A F *et al* 2004 *Preprint* cond-mat/0405264 1
[25] Anderson P W *et al* 2000 *Physica* C **9** 341
[26] Norrman M R *et al* 2002 *Phys. Rev.* B **66** 100506